

New Data Fusion Techniques for High-Precision Localization of Civil-Engineering Equipment

Ph. BONNIFAIT*, F. PEYRET**, G. GARCIA*

* Institut de Recherche en Cybernétique de Nantes (IRCyN) UMR 6597

1 rue de la Noë, BP 92101, 44321 Nantes cedex 03, France.

Tel: (33) 2-40-37-16-00; fax: (33) 2 -40-37-25-22;

e-mail: Philippe.Bonnifait@lan.ec-nantes.fr - Gaetan.Garcia@lan.ec-nantes.fr.

**Laboratoire Central des Ponts et Chaussées (LCPC)

BP 19, 44340 Bouguenais, France.

Tel: (33) 2-40-84-58-00; fax: (33) 2-40-84-59-99;

e-mail: Francois.Peyret@lcpc.fr.

Abstract

This paper presents two localization fusion techniques for civil-engineering machines. The first one concerns 2D localization and the second one is intended to 6 dof position and attitude determination. The system uses an optical instrument called SIREM which provides azimuth and elevation angles of known landmarks. The approach is based on dead-reckoning techniques updated by the exteroceptive measurements of SIREM using the Kalman filter formalism. As the dynamics and accelerations of the vehicles we consider are small enough, the use of inclinometers is attractive since they directly provide attitude angles. In such a context, we propose a new 3D dead reckoning method which integrates data from two inclinometers and an odometer. A large section of the paper is devoted to real experiments. These are performed with an outdoor tire-type robot moving on a 30x40 square meters non planar lawn. The results show that the precision of our system, although difficult to assert with the current experimental setup, is in the order of centimeters.

1. Introduction

Real-time positioning of civil-engineering mobile equipment such as dozers, motor graders, compactors, pavers, etc., can be of great interest for improving the global efficiency of the worksites. The huge technical gap existing between the high computerized design and the still archaic site works can be reduced by using in real-time the reference geometrical data for the control of the

mobile equipment. Significant improvements in terms of quality and saving of time and materials can be expected.

To solve this problem, several technologies can be addressed. The new Differential Global Positioning System seems to be a very promising solution fitting most of the earth-moving tasks. For the spreading tasks, the most demanding in terms of accuracy, optical technologies remain the most accurate.

Many researches have already been performed in order to design well adapted devices, in terms of accuracy, range, reliability, easiness of use and cost. Since 1990, the LCPC and the IRCyN have been developing a positioning prototype (SIREM), using standard light sources and a rotating linear CCD camera. SIREM measures the azimuth and elevation angles of known beacons.

This system has proved to be basically accurate enough but suffers from some structural drawbacks. One of these is the low rotation speed (imposed by the CCD technology and the required accuracy) which leads to a low updating rate.

Moreover, due to this low acquisition frequency, the sensor does not lend itself to the use of the so-called "quasi-static" methods, in which several measures are supposed to have been acquired at the same position.

The paper is organized as follows. We first describe the principle of SIREM and present the experimental setup. The vehicle is an outdoor mobile robot with rubber tires, moving on a slightly irregular terrain (a lawn).

Section 3 is dedicated to a 2D fusion of SIREM and odometry. The Extended Kalman Filter (EKF) approach is described and real experiments show that our system reaches a precision of a few centimeters in x and y, and 0.5 degrees in heading.

In the context of some tasks, the elevation and the attitude angles are required. Therefore in section 4, another fusion is being studied, using two inclinometers added to the above-mentioned sensors. These inclinometers provide accurate information in relation with the third dimension, since the dynamics of the vehicle are sufficiently low. In order to exhibit the inclinometer measurements, we propose a non-usual attitude representation based on the use of the gradient and cross-slope angles. We then propose a new 3D dead-reckoning technique on which an EKF is based. Very encouraging simulation show that the precision of the elevation estimation can reach one centimeter. Finally, the first outdoor experiments, carried out on a special test-track, are reported and analyzed in comparison with a Differential GPS RTK.

2. Sensors and experimental setup

2.1 SIREM: the exteroceptive sensor

Placing easy-to-recognize beacons in the environment of the robot is an effective way of avoiding many of the problems associated with recognizing natural landmarks. The artificial beacons we use are battery-powered twin light sources. A beacon is automatically switched on using an HF link, just before the rotational sensor is going to detect it. Once the reading is done, the light is switched off in order to decrease energy consumption.

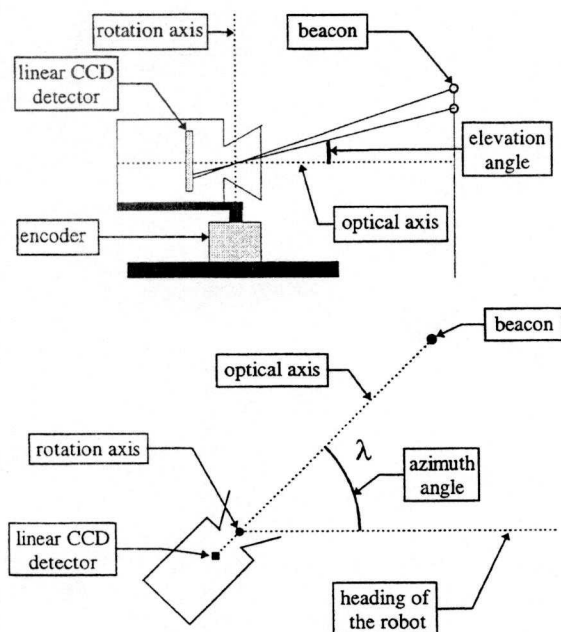


figure 1: side and top views of SIREM

SIREM is a linear CCD camera which rotates with a constant speed (≈ 1 rad/s) around an axis fixed to the

vehicle. Hence, the landmarks are detected one at a time and intermittently.

The rotation axis passes through the optical center (figure 1). The azimuth angles (denoted λ) are measured with respect to the heading by an optical encoder. The accuracy of this measurement depends on the scanning frequency of the camera and on the rotation speed. The low speed we have chosen provides accurate angles (the standard deviation of an azimuth angle is $2.2 \cdot 10^{-3}$ rad).

The sensor is also able to measure simultaneously the angle between the camera optic axis and the line that passes through the optical center and the beacon. This angle is called "elevation angle".

A particular problem of this kind of sensors is that it provides asynchronous measurements. Asynchronous means that the time of the detection of a beacon cannot be known beforehand, since, for a given position of the beacons, the angular interval between two beacons depends on the position and movement of the mobile.

2.2 The complete system

A good way for overcoming this drawback is data fusion between low-frequency optical measurements and high rate dead-reckoning or inertial measurements. We propose to study how some low-cost sensors can improve both updating frequency and global reliability, together with the accuracy.

Odometric techniques can be realized using optical encoders mounted directly on two wheels of the vehicle and two inclinometers. We suppose in this article that the outdoor vehicle has tire wheels, but our algorithm can be applied to caterpillar machines.

In order to measure the gradient and the cross-fall (denoted respectively "dc" and "dv"), pendulous inclinometers can be of great interest and the precision can be better than 0.1 degrees.

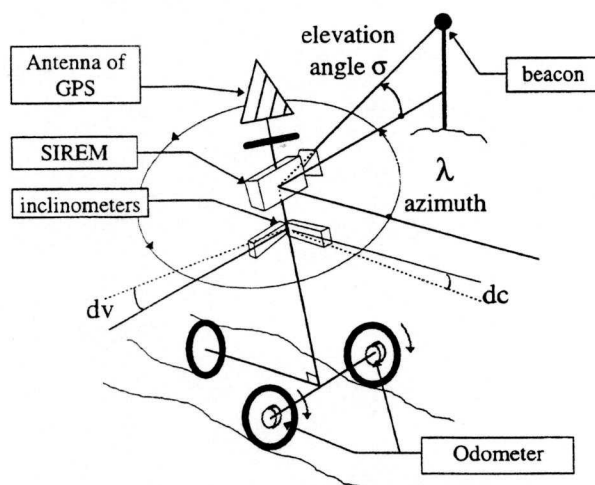


figure 2: the complete experimental setup on the vehicle

The recent advances in Differential GPS seem to provide enough accuracy for a significant number of applications. In order to compare the behavior of a Differential GPS RTK (Real Time Kinematic) and SIREM, we have installed a TRIMBLE 4000 GPS receiver on the experimental robot.

Finally, the disposition of the sensors on a two-wheeled mobile robot is shown on figure 2.

3. 2D fusion of SIREM and odometry

We first addressed 2D positioning; The basis of the solution was to correct odometric estimates using the azimuth angle measurements of SIREM. The improvement of the 2D parameters, x , y and direction angle (θ) is significant.

3.1 State-space description and Kalman filtering

The posture (position and orientation) of the vehicle at time instant i , can be represented in a two-dimensional space by the vector $X_i = [x_i \ y_i \ \theta_i]^t$.

Odometric equations provide a kinematic evolution model (see [3]). The odometer measures the vector $U_i = [\Delta_i, \omega_i]^t$ which is the elementary translation and rotation applied to the vehicle.

$$X_{i+1} = F(X_i, U_i) \quad (1)$$

The observations are the azimuth angles λ_j of the landmarks B_k , the coordinates of which are denoted (x_{B^k}, y_{B^k}) . The observation equation is **scalar**, but **non-stationary** since it depends on the coordinates of the landmark sensed.

Suppose this measurement occurs at time instant j ; figure 1 yields:

$$\lambda_j = \text{atan2}(y_{B^k} - y_j, x_{B^k} - x_j) - \theta_j = g^k(X_j) \quad (2)$$

Equations (1) and (2) are actually corrupted by noises which are supposed to be zero-mean, white and Gaussian. The system obtained is **non-linear** and has the following state-space description:

$$\begin{cases} X_{i+1} = F(X_i, U_i) + \alpha_i \\ \lambda_j = g^k(X_j) + \beta_j \end{cases} \quad (3)$$

α_i is the model noise which represents the effect of slippage or skid on the ground plus the effects of errors on the robot parameters such as the radii or the wheel base. β_j is a white noise due to measurement errors on the azimuth.

One can notice that the state-space description has two time indexes i and j . The last one indicates that the goniometric sensing are done asynchronously and intermittently.

Because of the non-linearity, we use an EKF to estimate the state X . The linearized state description uses Jacobian matrices.

$$\begin{cases} X_{i+1} = \left[\frac{\partial F}{\partial X} \right]_{\hat{X}_{i+1}} \cdot X_i + \left[\frac{\partial F}{\partial \Delta q} \right]_{\Delta q_i} \cdot U_i + \alpha_i \\ \lambda_j = \left[\frac{\partial g^k}{\partial X} \right]_{\hat{X}_{i+1}} \cdot X_j + \beta_j \end{cases} \quad (4)$$

Classical EKF computations are applied on system (4). The algorithm works in two steps: prediction and filtering.

Between two absolute readings, a "high" frequency (20 Hz, as compared to the frequency of the absolute readings ≈ 0.5 Hz) state and error prediction phase occurs. In this step a predicted state and its estimated error covariance matrix are computed.

When a beacon is detected, the posture is corrected: this is the filtering phase. Equation (5) shows that the prediction state is corrected proportionally to the difference between the measured azimuth angle λ_j and the expected azimuth angle $\hat{\lambda}_j$. Thanks to the Kalman gain vector K_j a scalar term is able to correct the three-dimensional vector X .

$$\hat{X}_{j+1/j+1} = \hat{X}_{j+1/j} + K_j \cdot (\lambda_j - \hat{\lambda}_j) \quad (5)$$

In the following, we will denote by "EKF_2D" the localization system based on EKF using SIREM and odometry.

3.2 Comments on the number of beacons

Although three beacons are necessary to localize a motionless vehicle, our system is able to work when the vehicle detects only two beacons while moving, except on some degenerate trajectories which have been determined thanks to observability analysis [4]. In practice, this is an interesting feature of our solution since, for instance, another vehicle can hide accidentally a landmark. Moreover, it helps reducing the number of beacons and hence the cost of the infrastructure.

3.3 Experimental results

In this section, we report the results of real-time experiments carried out with a 486-based PC system. Thanks to a real-time executive, periodic readings of the encoders, computation of the asynchronous azimuth angles from the CCD camera, lighting and extinction of the beacons, and all the computations of the estimation process, are done in real time.

The experiments have been run on an outdoor test-track marked out with three beacons (see figure 3), with a

three-wheeled, non-holonomic vehicle (figure 4). Reference points have been located by surveyors, in a local frame. White strings can be stretched out on the grass to materialize straight lines or circles of known equations.

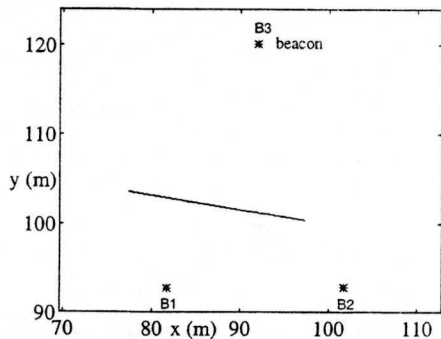


figure 3: experimental path

The principle of our experiments is to make the robot track those reference paths using a CCD camera (see the picture of figure 4), and to compare the EKF estimation results with reality. The camera, at the front of the robot, extracts the deviation between its optical axis and the white line to be tracked. The global accuracy of the tracking process can be estimated around ± 1 cm, at a speed of 10 cm/s.

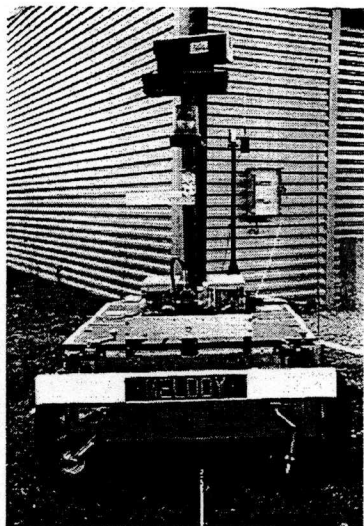


figure 4: the experimental robot

In the experiments, we also store the location data provided by the Differential GPS RTK. Since we have calibrated the relative positions of the sensors, we can compare the locations computed by each system (the locations of the GPS are converted in the local frame).

In the reported test (figure 5), the robot tracks a straight line (speed ≈ 6 cm/s) of known equation, so we can compute the lateral errors. One can notice that we compute this error while the vehicle is moving. Before the robot moves, the filter is initialized using a deterministic iterative method presented in [9].

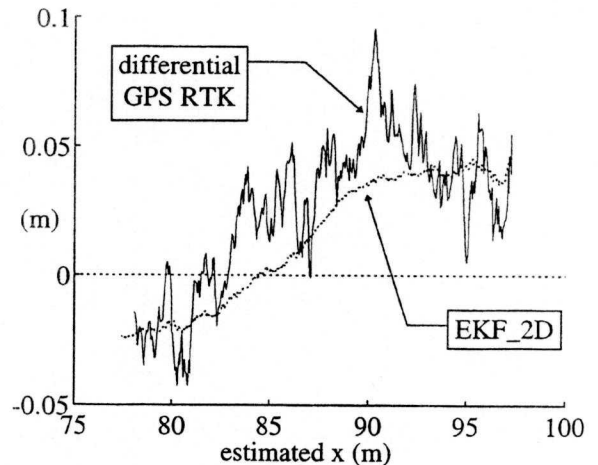


figure 5: Signed lateral errors

One should keep in mind that the accuracy of the reference marks and beacons positioning is about one centimeter. Moreover, it's difficult to guarantee that the string is perfectly stretched out and the robot, when following the line, oscillates a little.

The results of figure 5 prove that the EKF_2D and the GPS provide very good position measurements, in the same range of accuracy. One can notice that the estimations of EKF_2D are less noisy.

Nevertheless, the lateral errors don't have zero means and are not random signals due to measurement noises only. Most probably, it is largely due to the terrain generating the same roll angle at each test. Indeed, the sensor is located about 1.9 m above the ground (see figure 6). Hence, one degree of cross-fall generates a three-centimeter lateral error (our test-track is a lawn and not perfectly planar). Repeatability tests (cf. [3]) confirm this phenomenon.

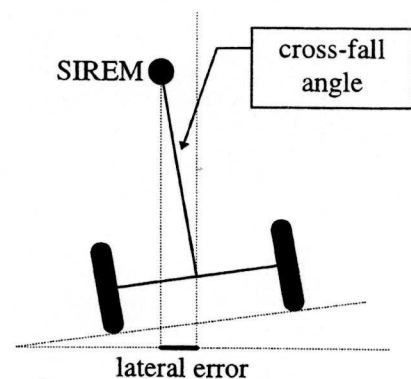


figure 6: effect of a non modeled cross-fall angle

Since one of the two inclinometers directly measures the cross-fall angle, we can verify this explanation. Indeed, as shown on figure 7, the shape of the signal perfectly corresponds to the lateral error of figure 5.

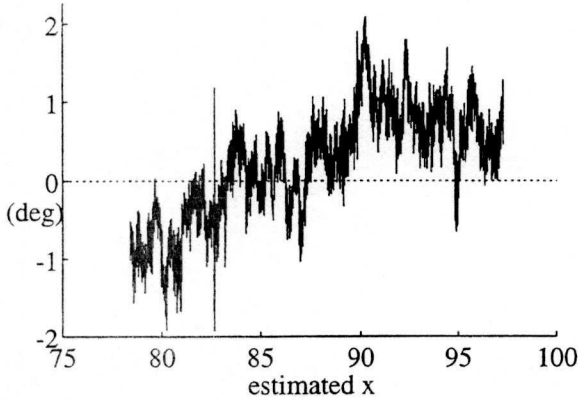


figure 7: output signal of the cross-fall inclinometer

The current experimental setup does not allow to assert the precision of our system. A special test track is necessary for precision tests. Such a facility called "SESSYL" is available by the LCPC. SESSYL is a robotized head with three degrees of freedom mounted on a carriage that moves along a calibrated rail.

4. 3D fusion of SIREM, odometry and inclinometers

4.1 Choice of the state vector

In general, six independent variables are required to describe the posture (position and attitude) of a solid. Usually, position is given by the Cartesian coordinates, but as regards the attitude many representations can be used. For instance, rotation matrices are given by roll-pitch-yaw angles [8, 11, 12] or Euler angles [1]. These transformations have singularities but need only three parameters. On the other hand, quaternions [10] provide non-singular representations, but with four parameters.

We propose to use a geometrical parametrization which is defined by the direction angle ψ , the gradient (dc) and the cross-fall (dv) (see figure 8) which are directly measured by the inclinometers. The attitude matrix 0A_S is a function of ψ , dc and dv. Its expression is given in [5].

If we compare with the "yaw-pitch-roll" rotation matrix (in this order), we have Ψ = yaw, dc = pitch and:

$$\tan(dv) = \tan(\text{roll}) / \cos(\text{pitch}) \quad (6)$$

One can notice that the gradient and the cross-fall are not defined for $\pm\pi/2$. These situations never occur in realistic situations.

As we use the Cartesian position, the state vector we propose to estimate is:

$$X = [x \ y \ z \ \psi \ dc \ dv]^T \quad (7)$$

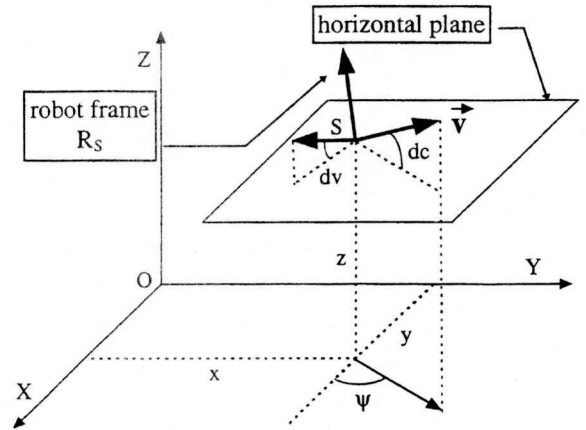


figure 8: choice of the six independent parameters

This state vector perfectly defines the robot frame denoted R_S (figure 8).

4.2 Odometry on a non-planar surface with two inclinometers

When moving on a non-planar surface, the posture of a mobile changes in three dimensions.

Fuke and Krotkov [8] use encoders to calculate the velocity. By EKF, they combine three gyros and three accelerometer signals and determine the attitude. Then, they incrementally update the position. The approach we propose uses only four sensors: two encoders and two tilt sensors.

Suppose X_i , the state vector at time i , is known. We want to compute X_{i+1} , knowing $U_{i+1} = [\Delta_{i+1}, \omega_{i+1}]^T$ the elementary translation and rotation measured by the odometer between times i and $i+1$, and $(\alpha_{i+1}, \beta_{i+1})$ the measurements of the two inclinometers at time $i+1$.

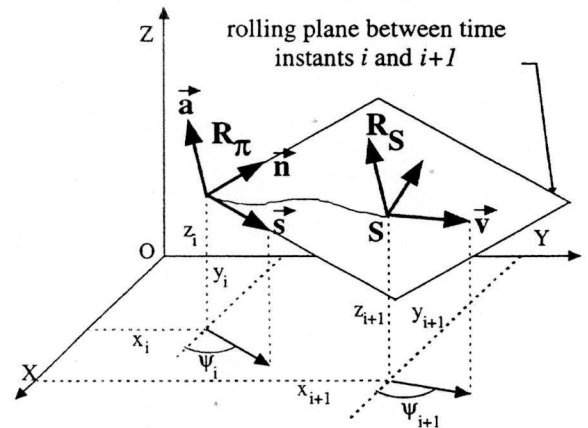


figure 9: elementary motion in the plane defined by the last estimated position and the inclinometers

We use an auxiliary frame, denoted R_π such that $(R_s)_i = (R_\pi)_i$. At time i , the origin Ω of R_π is equal to point S , origin of R_s . Nevertheless, while the robot moves between time indexes i and $i+1$, the frame R_π remains motionless.

So, the problem is to determine the elementary variation of the state sub-vector $[x, y, z, \psi]^t$. The new values of dc and dv are directly given by the inclinometer measurements (α, β) .

$$\text{in } R_0 \begin{cases} x_{i+1} = x_i + \delta x(X_i, U_{i+1}) \\ y_{i+1} = y_i + \delta y(X_i, U_{i+1}) \\ z_{i+1} = z_i + \delta z(X_i, U_{i+1}) \\ \psi_{i+1} = \psi_i + \delta \psi(X_i, U_{i+1}) \\ dc_{i+1} = \alpha_{i+1} \\ dv_{i+1} = \beta_{i+1} \end{cases} \quad (8)$$

The elementary variations δx and δy in R_0 are computed using classical odometric equations [3] but in the rolling plane. To calculate the displacement, we suppose that the robot first performs a translation $\bar{\Delta}_T$ of length Δ_{i+1} and then rotates. Then, we project this equation in R_0 .

$$\begin{pmatrix} 0 \\ \Delta_T \end{pmatrix}_i = \begin{pmatrix} 0 \\ A_\pi \end{pmatrix}_i \cdot \begin{pmatrix} \pi \\ \Delta_T \end{pmatrix}_i \quad (9)$$

The first two components of $\begin{pmatrix} 0 \\ \Delta_T \end{pmatrix}_i$ give the variation on x and y in R_0 .

From the odometric measurements ω_{i+1} , we know the expression of the rotation vector $\bar{\Delta}_R$ in the frame $(R_\pi)_i$:

$$\begin{pmatrix} \pi \\ \Delta_R \end{pmatrix}_i = [0 \ 0 \ \omega_{i+1}]^t \quad (10)$$

Hence in R_0 :

$$\begin{pmatrix} 0 \\ \Delta_R \end{pmatrix}_i = \begin{pmatrix} 0 \\ A_\pi \end{pmatrix}_i \cdot \begin{pmatrix} \pi \\ \Delta_R \end{pmatrix}_i \quad (11)$$

The third component of $\begin{pmatrix} 0 \\ \Delta_R \end{pmatrix}_i$ is the projection of $\bar{\Delta}_R$ on the z_0 axis of R_0 and is the variation of ψ , $\delta\psi$. The exact expressions of δx , δy and $\delta\psi$ can be found in [5].

Finally, we suppose that there is no offset, between the gradient and cross-fall and their corresponding measurements given by the inclinometers. This supposes a good calibration of the system on the robot. Consequently, the plant model for the elevation is given by:

$$\delta z(X_i, U_{i+1}) = \Delta_{i+1} \sin(dc_i) \quad (12)$$

4.3 Recursive 6 dof estimation

The recursive state estimator we use is based on an Extended Kalman Filter (EKF) formulation.

The odometric measured speeds are seen as the control input to the mobile and, therefore, appear in the

prediction phase. As presented in a 2D case [3], we compute the prediction error using a linearized method.

A **synchronized estimation phase** is performed with the inclinometer data, whereas a second **intermittent correction phase** is done when the azimuth and elevation angles of a beacon are available. In average, this correction phase occurs every 40 prediction/estimation phases.

```

Begin
  Static localization (see [9]) - filter initialization
  Do
    U = read odometric data
    (X,P) = prediction phase(X,P,U)
    I = read inclinometers data
    (X,P) = estimation phase(X,P,I)
    if (external measure  $\Lambda$ ) do
      (X,P) = correction phase(X,P, $\Lambda$ )
    End if.
  End loop at the frequency of 20 hz
End.

```

The plant model of the prediction phase is adapted from equation (8), but the evolution model for dc and dv is a constant. Evolution is made possible by the model noise $[\alpha_{dc}, \alpha_{dv}]^t$. If the variance of this noise becomes small, the overall effect of the EKF for dc and dv is similar to a "low pass" filter applied to their measurements. This can be of great use, in real situations, to filter the vibrations induced by the engine.

$$\text{in } R_0 \begin{cases} x_{i+1} = x_i + \delta x(X_i, U_{i+1}) + \alpha_x \\ y_{i+1} = y_i + \delta y(X_i, U_{i+1}) + \alpha_y \\ z_{i+1} = z_i + \delta z(X_i, U_{i+1}) + \alpha_z \\ \psi_{i+1} = \psi_i + \delta \psi(X_i, U_{i+1}) + \alpha_\psi \\ dc_{i+1} = dc_i + \alpha_{dc} \\ dv_{i+1} = dv_i + \alpha_{dv} \end{cases} \quad (13)$$

$$\Leftrightarrow \{X_{i+1} = F(X_i, U_{i+1}) + \alpha_X \quad (14)$$

As soon as the prediction phase is done, the estimation phase is performed with the inclinometers. The observation equation is given by:

$$\begin{pmatrix} \alpha_i \\ \beta_i \end{pmatrix} = \begin{bmatrix} 0 & 0 & 0 & 0 & 1 & 0 \\ 0 & 0 & 0 & 0 & 0 & 1 \end{bmatrix} \cdot X_i = C \cdot X_i \quad (15)$$

One can notice that the Kalman formulation is linear in this step.

At time j , when an asynchronous optical measure occurs, the predicted sub-vector $[x, y, z, \psi]^t$ is corrected: this is the correction phase. Thanks to this step, estimation errors on these parameters do not drift.

In order to express the relations between the measurement angles (λ, σ) and the state X , we first need to determine the position of the beacon in the frame R_S of the exteroceptive sensor.

In R_0 , the known homogeneous position of the beacon is defined by:

$${}^0P_B = \begin{bmatrix} {}^0x_B & {}^0y_B & {}^0z_B & 1 \end{bmatrix}^t \quad (16)$$

Let 0T_S denote the homogeneous transformation matrix of the sensor frame relative to R_0 :

$${}^0T_S = \begin{bmatrix} x \\ {}^0A_s & y \\ z \\ 0 & 0 & 0 & 1 \end{bmatrix} \Leftrightarrow {}^0T_S = \begin{bmatrix} {}^0A_s & {}^0P_s \\ 0 & 1 \end{bmatrix} \quad (17)$$

In R_S , equation (16) becomes:

$${}^sP_B = {}^sT_0 \cdot {}^0P_B = \begin{bmatrix} {}^0A_s^t & -{}^0A_s^t \cdot {}^0P_s \\ 0 & 1 \end{bmatrix} \cdot {}^0P_B \quad (18)$$

Finally, the two observation equations (see figure 2) are given by:

$$\begin{cases} \lambda_j = \text{atan2}({}^s y_b, {}^s x_b) \\ \sigma_j = \arctan\left(\frac{{}^s z_b}{\sqrt{{}^s x_b^2 + {}^s y_b^2}}\right) \end{cases} \Leftrightarrow \begin{pmatrix} \lambda_j \\ \sigma_j \end{pmatrix} = G_b(X_j) \quad (19)$$

The subscript b of function G_b , means that these equations depend on the landmark which has been detected. Thus, the observation equation is, in this phase, unstationary.

The extended Kalman filter formulation is more detailed in [5]. In the following, we will denote by "EKF_3D" the localization system based on EKF using SIREM and 3D odometry.

4.4 Simulation results

Simulations have been performed with a specialized simulator for road construction [2] based on Matlab and Simulink. Gaussian random noises have been added to the measurements. In particular, the variance of the errors of the inclinometers has been multiplied by two, in order to compensate for the effects of the vibrations and accelerations of the machine. Noise variances for the goniometric sensor and for the encoders are those of the real sensors, already used in [3].

4.4.1 Real trajectory

The real trajectory corresponds to the curves of figure 10, with a constant projected speed of 0.1 m/s, in (O, x_0, y_0) .

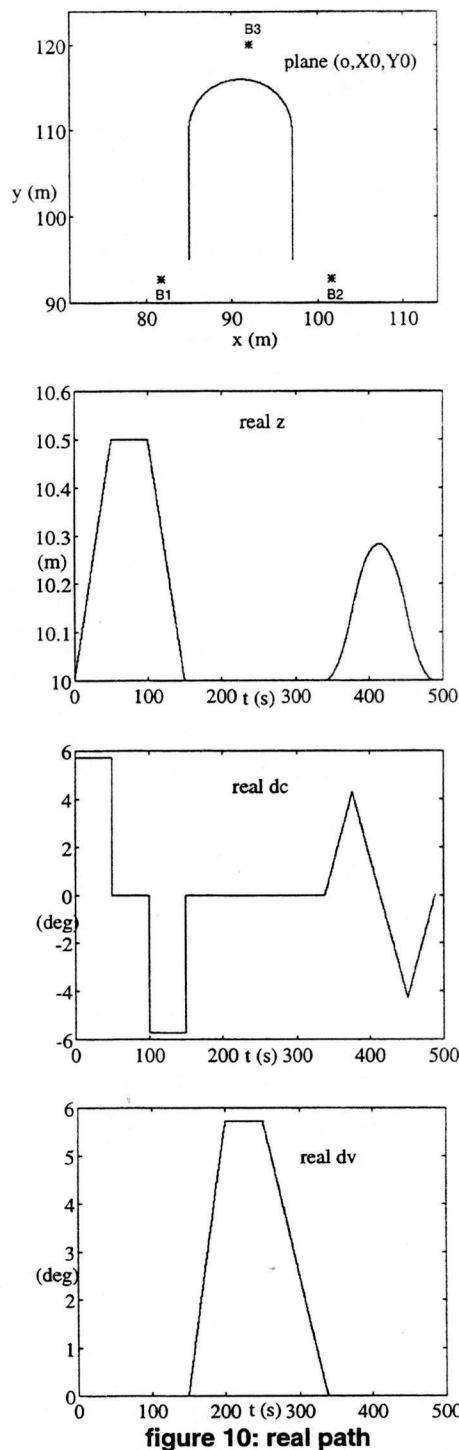


figure 10: real path

The projected path of figure 10 is made up of a straight line, a semicircle and a straight line. The altitude, dc and dv are functions of the curvilinear abscissa in (O, x_0, y_0) . During the first line, the elevation follows a linear variation, whereas after the semicircle, the variation is parabolic. Finally, the cross-section is horizontal, except in the half circle.

The principle of the simulation is to have a modeled robot which follows this 3D path. While moving, inclinometer and odometric measurements are calculated. The rotation of the camera is also modeled, therefore, the asynchronism of the azimuth and elevation angles is taken into account.

4.4.2 State estimation analysis

Even if the EKF is initialized with significantly large errors (50 cm error on xy, 15 cm on z, 2 degrees on Ψ and 1 degree on dc and dv), the transient phase is short, as shown on figure 11.

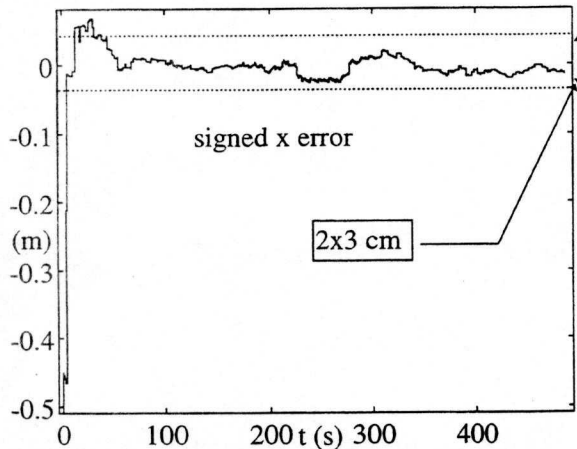


figure 11: abscissa error of EKF_3D

The 2D behavior, i.e. the sub-vector $[x, y, \psi]^t$ is close to the one we have encountered with real data in section 3. The distance error is in the order of a few centimeters and the heading error standard deviation is equal to 0.4 degrees.

The global estimation process has a good behavior since errors have zero means. Moreover, they are far lower than one estimated standard deviation, as exemplified by figure 12. This behavior indicates a good EKF process.

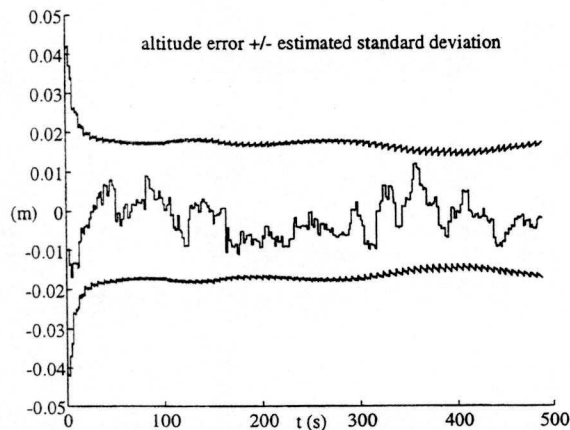


figure 12: signed altitude error and estimated standard deviation of EKF_3D

On figure 12, the zero mean elevation error remains bounded by 1 cm. Its shape does not depend on the longitudinal-section, or on the cross-section. This proves that the 3D odometric evolution is good.

Simulations clearly indicate that the filtering of the inclinometers is of particular importance since, in addition to reducing errors on dc and dv, it also significantly improves the elevation estimation. Indeed, oscillations and peaks are filtered. This is an interesting aspect of our filter: the integrated "low pass" filter on dc and dv, also filters the z estimation.

4.5 First experimental results

Real experiments have been performed in a lawn, with a special test-track. This equipment is an adjustable bridge on which the robot moves. Its length is approximately 7 m and the maximum elevation is 0.4 m. The principle of the experiments is the same as the one of section 3.3: the mobile robot still tracks the white line with a constant speed of 6 cm/s. Nevertheless, in these tests, sensor data are stored and the fusion process is performed by post-processing.

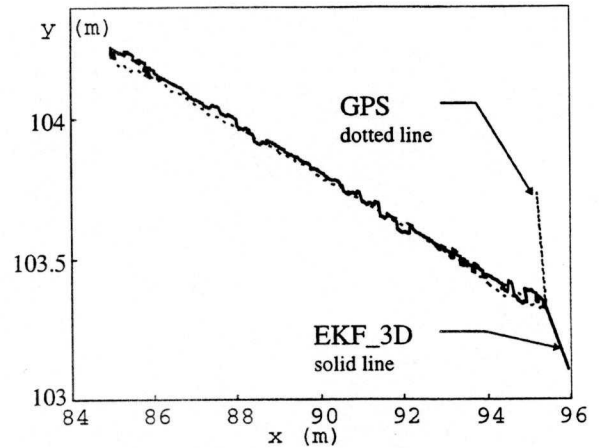


figure 13: estimated paths in (o, X_0, Y_0)

The initial error of EKF_3D is due to the iterative deterministic method which initializes the algorithm: the convergence toward the real position is then fast.

The GPS large error is more difficult to analyze since we don't know if it is the result of a trouble with the radio link with the fixed station or if it is a consequence of a changing of satellites.

The same comments can be done for the elevation initial errors on figure 14.

On figure 13, we can notice that both systems have a precision better than 10 cm: the oscillations are more or less the same.

Concerning the elevation estimation, it appears that when moving, EKF_3D is very sensitive to the transient phases caused by the short slopes (figure 14): elevation

error can be up to 10 cm. On the contrary, the dynamics of the vehicle seems to poorly affect the GPS behavior, as predictable.

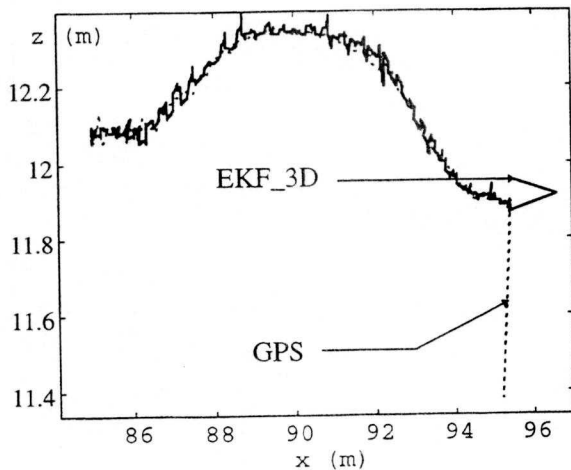


figure 14: estimated altitudes

When the robot is motionless, the precision of EKF_3D seems to be in the order of few centimeters as indicated by figure 15.

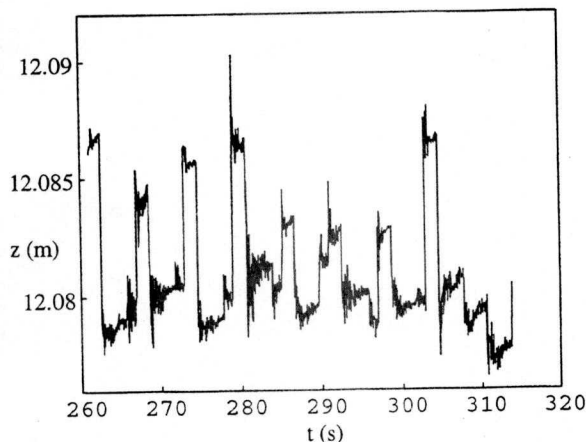


figure 15: estimated altitude by EKF_3D when the robot is motion-less

These results have to be analyzed carefully since the algorithm of EKF_3D does not take into account the translation between the odometric center and the camera of SIREM. Consequently, in this experiment the slopes produce undesirable transient phases.

Moreover, as shown by the simulations of section 4.4, the z estimation process is very sensitive to calibration error between the frame of SIREM and the inclinometers. For instance, an offset of 0.01 degrees induces 7 mm oscillations on z , if the distance between the beacons and the sensor is superior to 40 m.

A good dc and dv estimation is a second crucial parameter. This involves to correctly filter the noisy

outputs of the inclinometers. Nevertheless, a too strong low pass filtering generates a difference in phase which induces oscillations in z during the transient phases. A good compromise is shown on figure 16 and figure 17.

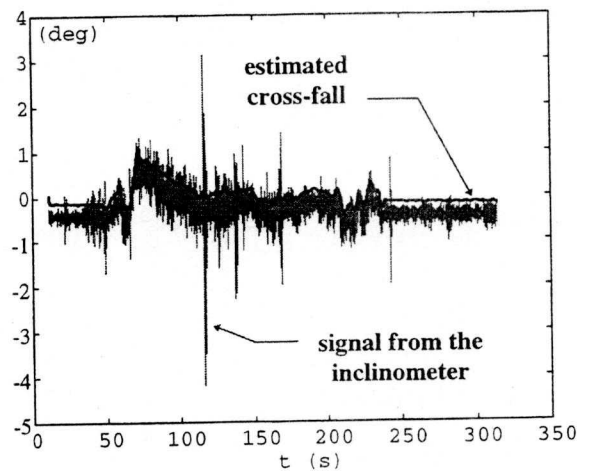


figure 16: estimated cross-fall and raw signal of the inclinometer

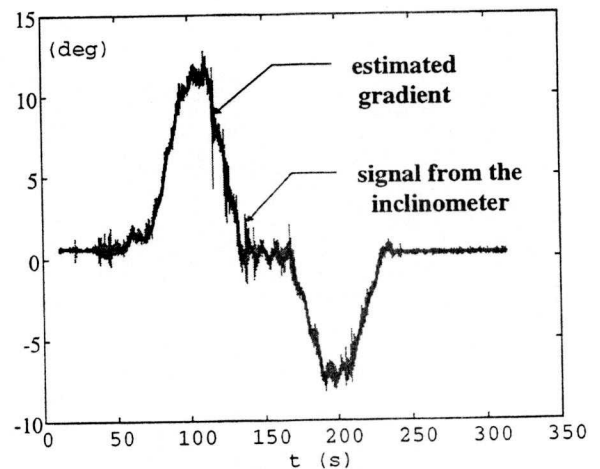


figure 17: estimated gradient and raw signal of the inclinometer

The outputs of the inclinometers are sufficiently filter since the oscillations on the estimations are less than 0.1 degrees. Moreover, the offset between SIREM and the cross-fall inclinometer is clearly visible on figure 16.

5. Conclusion and future work

In this paper, we have presented two localization systems based on the fusion of dead-reckoning and exteroceptive goniometry.

Extensive outdoor tests have been performed in real conditions. They indicate that the precision of the 2D

fusion method of SIREM and odometry is in the order of centimeters.

Moreover, in order to extend this approach to the 3D case, we have presented 3D-odometric equations. Our formalism uses only four sensors: two inclinometers and two encoders. The experimental results prove that the non modeled accelerations deteriorate little or not the inclinometer measurements, which validates our approach.

The update of this 3D dead-reckoning position estimation is performed by an EKF which allows to take into account each goniometric measurement individually and asynchronously. The estimated state we have chosen exhibits the tilt sensor measurements thanks to a non usual attitude representation in robotics, based on the cross-fall and gradient angles.

Simulations and real experiments indicate that the elevation estimation is very sensitive to the noise of the inclinometer. A good filtering of inclinometer data is of great use for the elevation estimation.

Moreover, when the z evolution is slow, the altitude accuracy is better than a few centimeters. Oscillations appear when the altitude changes quickly, but an EKF divergence has never been noted.

Finally, we have compared our fusion method with a Differential GPS RTK. The precision seems to be in the same order in the two cases. Our belief is that these two systems are complementary. Indeed, the main drawback of SIREM is that it requires precise positioning of the beacons. On the other hand, GPS suffers from shadowing which occurs under bridges for instance. Our system is an alternative to GPS in such situations.

Future work involves a better calibration of the system. Finally, as the 3D estimation process is twice slower than the 2D filter, simplifications have to be considered in order to implement the method in real time.

REFERENCES

- [1] B. Barshan et H.F. Durrant-Whyte. "Inertial navigation systems for mobile robots". *IEEE Transactions on Robotics and Automation*. Vol. 11, n°3, June 1995, pp 328-342.
- [2] D. Bétaille, F. Peyret, "A simulator for road construction equipment", ISARC 97, Pittsburgh.
- [3] Ph. Bonnifait and G. Garcia, "A multisensor localization algorithm and its real-time experimental validation". *IEEE Int. Conf. on Robotics and Automation*, pp 1395-1400. Minneapolis, April 1996.
- [4] Ph. Bonnifait and G. Garcia. "On the use of non-linear conditions in determining test situations for a mobile robot localizer". *World Automation Congress. International Symposium on Robotics And Manufacturing*. Montpellier, May 1996.
- [5] Ph. Bonnifait and G. Garcia "Dynamic determination of the 6 dof of a mobile robot using odometry, inclinometers and a goniometric system", Syroco Nantes, September 1997. (to appear).
- [6] R. G. Brown et P. Y.C. Hwang. "Introduction to random signals and applied Kalman filtering". Second edition. Wiley 1985.
- [7] J.-H. Chen, S.C. Lee et D. B. Debra. "Gyroscope free strapdown inertial measurement unit by six linear accelerometers". *Journal of guidance, control and dynamics*. Vol. 17, n°2, March -April 1994, pp 286-290.
- [8] Y. Fuke et E. Krotkov. "Dead reckoning for a lunar rover on uneven terrain". *IEEE Int. Conf. on Robotics and Automation*. Minneapolis. April 1996. pp 441-416.
- [9] J.-F. Le Corre and G. Garcia, "Real-time determination of the location and speed of mobile robots running on non-planar surfaces". *IEEE Int. Conf. on Robotics and Automation*. Nice, May 1992. pp 2594-2599.
- [10] K. Rintanen, I. Kauppi, K. Koskinen, A. Koskinen. "Inertial navigation for mobile robots by redundant low-cost gyrometers". *Tampere Int. Conf. on machine automation*. Tampere, February 1994. pp225-241.
- [11] T. Tsumura, H. Okubo et N. Komatsu. "A 3D position and attitude measurement system using laser scanners and corner cubes". *IEEE/RSJ Int. Symp. on Intelligent Robots and Systems*. Yokohama 1993. pp 604-611.
- [12] J. Vaganay, M.J. Aldon and A. Fournier, "Mobile robot attitude estimation by fusion of inertial data", *IEEE Int. Conf. on Robotics and Automation*, Atlanta, May 1993. pp 277-282.